Advances in Materials Research, *Vol. 4, No. 3 (2015) 145-164*
DOI: http://dx.doi.org/10.12989/amr.2015.4.3.145

Biophysical properties of PPF/HA nanocomposites reinforced with natural bone powder

Nagwa A. Kamel[*1], Samia H. Mansour[2], Salwa L. Abd-El-Messieh[1], Wafaa A. Khalil[3] and Kamal N. Abd-El Nour[1]

[1]*Microwave Physics and Dielectrics Department, National Research Centre, Dokki, Cairo, Egypt,*
[2]*Polymers and Pigments Department, National Research Centre, Dokki, Cairo, Egypt*
[3] *Biophysics Department, Faculty of Science, Cairo University, Egypt*

(Received March 19, 2015, Revised November 16, 2015, Accepted November 16, 2015)

Abstract. Biodegredable and injectable nanocomposites based on polypropylene fumarate (PPF) as unsaturated polyester were prepared .The investigated polyester was crosslinked with three different monomers namely N-vinyl pyrrolidone (NVP), methyl methacrylate (MMA) and a mixture of NVP and MMA (1:1 weight ratio) and was filled with 45 wt% of hydroxyapatite (HA) incorporated with different concentrations of chemically treated natural bone powder (NBP) (5, 10 and 15 wt%) in order to be used in treatment of orthopedics bone diseases and fractures. The nanocomposites immersed in the simulated body fluid (SBF) for 30 days, after the period of immersion in-vitro bioactivity of the nanocomposites was studied through Fourier transform infrared (FTIR), scanning electron microscope (SEM), energy dispersive X-ray (EDX) in addition to dielectric measurements. The degradation time of immersed samples and the change in the pH of the SBF were studied during the period of immersion.

Keywords: biodegradable polyester; nanocomposites; bone powder; dielectric spectroscopy; biophysical properties

1. Introduction

Tissue engineering is a fast growing area of research that aims to create tissue equivalents of blood vessels, heart muscle, nerves, cartilage, bone and other organs for replacement of tissue either damaged through disease or trauma (Langer *et al.* 1993, Ma 2004, Ma 2005). Various materials have been used as scaffolds for tissue regeneration. Polymers have great design flexibility because the composition and structure that can be tailored to the specific needs and therefore have been extensively studied in various tissue engineering applications including bone tissue engineering (Ma 2008). The most common biodegradable polymers for bone grafts include poly (glycolic acid) (PGA), poly(lactic acid) (PLA) poly (lactic glycolic acid) (PLGA), poly(caprolactone) (PCL), poly (propylene fumarate)(PPF) and poly (ethylene glycol)(PEG).

Polymers usually do not me*et al*l the needs for various tissue engineering applications so most of the polymer based composite materials are designed to provide improved mechanical properties

∗Corresponding author, Professor, E-mail: nagwakamel@gmail.com

http://www.techno-press.org/?journal=amr&subpage=7 ISSN: 2234-0912 (Print), 2234-179X (Online)

such as strength, stiffness, toughness and fatigue resistance. Therefore, they are frequently used as biomaterials for orthopedic applications where mechanical properties are a serious concern.

One of these polymers that investigated as an injectable and biodegradable bone cement is poly (propylene fumarate) (PPF) (Lee *et al.* 2008a, Lee *et al.* 2008b) Studies have demonstrated that PPF scaffolds can be mechanically reinforced through the incorporation of nanoparticles and nanotubes to form nanocomposites. The inclusion of surface-modified carboxylate alumoxane nanoparticles (1 wt %) dispersed within PPF/PF-DA has been shown to result in a greater than 3-fold increase in flexural modulus compared to the PPF/PF-DA material alone (Horch *et al.* 2004). Further, increasing degrees of nanoparticle loading into the material did not result in significant loss of flexural or compressive strength (Horch *et al.* 2004, Shi *et al.* 2006, Temenoff *et al.* 2007).

Polymeric networks of poly (propylene fumarate) (PPF) crosslinked with poly (propylene fumarate)-diacrylate were investigated by Timmer *et al.* (2003) as an injectable, biodegradable bone cement. The effect of crosslinking density, medium pH, and the incorporation of beta-tricalcium phosphate (beta-TCP) filler on the in-vitro degradation of PPF/PPF-DA was studied. The results showed that the degradation of PPF/PPF-DA networks can be controlled by the crosslinking density, accelerated at a lower pH, and prolonged with the incorporation of the beta-TCP filler.

Jayabalan *et al.* (2011) studied the effect of hydroxyapatite (HAP) on the performance of nanocomposites of unsaturated polyester, i.e., hydroxy-terminated high molecular weight poly(proplyenefumarate) (HT-PPFhm), The tissue compatibility and osteocompatibility of the nanocomposite containing calcined HAP nanoparticles was evaluated. The tissue compatibility was studied by intramuscular implantation in a rabbit. They concluded that, the nanocomposite containing calcined HAP nanoparticles is both biocompatible and osteocompatible.

In our previous work (Kamel *et al.* 2012) polypropylene fumarate (PPF) crosslinked with NVP, MMA and NVP/MMA and filled with 40, 45 and 50 wt% HA was studied as biodegradable polyester nanocomposites to be used as bone substitute material. Results indicated that, the degradation rate decreases with increasing the HA content, the values of the compressive strength increased by increasing the filler content. The bioactivity of the nanocomposites was confirmed by different tools such as; Fourier transform infrared (FTIR), scanning electron microscope (SEM), energy dispersive X-ray (EDX) and dielectric spectroscopy.

In order to design composite biomaterials or to develop already existing composites for the repair of bone and cartilage, we need to consider and compare the structure and properties of these nanocomposites with those of the natural tissue (Gaharwar *et al.* 2011)

Natural bone matrix is a typical example of organic/inorganic composite material consisting of collagen and mineral (apatite). This natural composite material has an excellent balance between strength and toughness, superior to either of its individual components (Ma 2008). Previous works have highlighted the important role of the organic matrix on the mechanical properties of the whole bionanocomposites (Fantner *et al.* 2004). A variety of methods have been used to produce powders from bone (Johnson *et al.* 2000).

The aim of the present work is to modify the previous studied PPF/HA nanocomposites by incorporation of different concentrations of natural bone powder (5, 10 and 15wt %). The dielectric and mechanical properties of the new nanocomposites before and after immersion in simulated body fluid (SBF) will be studied. The in-vitro bioactivity will be also studied through the Fourier transform infrared (FTIR), scanning electron microscope (SEM), energy dispersive X-ray (EDX). The effect of introducing natural bone powder on the biodegradation rate and the change in pH during immersion in simulated body fluid (SBF) will be taken into consideration.

2. Materials methods

2.1 Materials

Diethyl fumarate, 1, 2-propanediol and tetrabutyl titanate as the transesterification catalyst were reagent grade from Merck, Darmstadt, Germany. N-vinyl pyrrolidone (NVP; freshly distilled) and methyl methacrylate (MMA; freshly distilled) were obtained from Merck, Darmstadt, Germany. Benzoyl peroxide, N, N-dimethyl-4-toluidine and hydroxyapatite were obtained from Sigma-Aldrich (Germany).

2.1.1 Synthesis of fumarate polyester resin

Polypropylene fumarate (PPF) was prepared by the two-stage melt polycondensation method (esterification and polycondensation) of (1 mol) diethyl fumarate and (2.2 mol) 1, 2-propanediol in the presence of catalyst. The detailed of preparation and characterization of PPF were described elsewhere (Kamel *et al.* 2010).

2.1.2 Crosslinking of the prepared fumarate polyester

Fumarate polyester resin (PPF) was crosslinked with 30% by weight of (N-vinyl pyrrolidone (NVP) or methyl methacrylate or a mixture of (NVP/MMA) in the ratio of 1:1 by weight using benzoyl peroxide as initiator (2% w/w).N,N-dimethyl-4-toluidine (0.2%) was added with rapid stirring, then the mixture was molded using appropriate molds for different tests. Curing occurred at room temperature (25^{o}C) for 24 h.

2.1.3 Preparation of natural bone powder

The natural bone powder was prepared from freshly removed diaphyses of the calf long bones. Bones were dissected from the surrounding connective tissues then alkali treated to leave the purely osseous structure free from all traces of tissues, fat or any organic matter occupying the intraosseous spaces. In alkali treatment, the bones were broken into small pieces and boiled for hours in a 30% sodium carbonate solution followed by thorough washing with hot water. The cycle of alkali treatment was currently repeated till constant weight was reached .The treated bones were then dried at 100^{o}C overnight and grounded to fine powder in a hardened steel vial. The bone powder was sieved to obtain suitable particle size (Moharram *et al*. 2007).

2.1.4 Fumarate polyester nanocomposites

The nanocomposites were prepared by mixing 45 wt% HA containing different concentrations of natural bone powder (5, 10 and 15 wt %) with a mixture of fumarate polyester resin and crosslinking agents namely NVP, MMA, and a mix of NVP/MMA in the ratio of 1:1 by weight. All the samples were left for 24 h at 25°C for curing.

2.2 Characterization techniques

2.2.1 Transmission electron microscope (TEM)

The particle size of HA and NBP was determined using transmission electron microscope model: Tecnai G 20, Super twin, double tilt and Magnification range up to 1,000,000 xs and applied voltage200 kV. Gun type: LaB6Gun Japan.

2.2.2 Scanning electron microscope (SEM), energy dispersive X- ray (EDX)

Morphology of the composite before and after soaking in SBF was studied through scanning electron microscope coupled with energy dispersive X-ray microanalysis (SEM/EDX, Philips XL30) Japan.

2.2.3 Fourier transform infrared (FTIR)

The infrared spectrum was recorded by a JASCO FT/IR 300 E Fourier Transform Infrared (FTIR) Spectrometer (Tokyo, Japan).

2.2.4 Dielectric measurements

The dielectric measurements were carried out in the frequency range 100 Hz up to100 kHz using an LCR meter, type AG-411 B (Ando electric, Japan). The capacitance C, loss tangent tan δ, and AC resistance R_{ac} were measured directly from the bridge from which the permittivity ε′, dielectric loss ε", and R_{dc} were determined. A guard ring capacitor type NFM/5T Wiss Tech. Werkstatten (WTW) GMBH Germany was used as a measuring cell. The cell was calibrated using standard materials and the experimental error in ε′and ε"were found to be ±3% and ±5%, respectively. The temperature was controlled to 30^{o}C by putting the cell in a digital oven and the experimental error in the temperature was ±0. 1°C.

2.2.5 In-vitro tests

To assess in- vitro bioactivity, the nanocomposites were soaked in simulated body fluid (SBF) at 37˚C for 30 days, after which they were rinsed gently with deionized water and dried. The disks were accurately weighed before and after immersion in SBF. The weight loss (WL) was calculated according to:

$$WL\% = (W_{0}\text{-}W_{d})/W_{d}\times 100$$

Where W_o the initial weight of the specimen and W_d the weight of the specimen dried after different degradation times (7, 14, 21 and 28 days). All the measurements were taken in triplicate and the average values were calculated.

2.2.6 pH measurements

The pH values were measured during soaking in SBF and readings were taken in an mPA-210 pH meter at 37˚C.

3. Results and discussion

3.1 Transmission electron microscope (TEM)

Fig. 1 gives a TEM micrograph of the hydroxyapatite particles used in this study .The image show that the sample exhibit needle like morphology. The particle size was found to be in the range of (26 -120) nm. These results are in good agreement with the HA micrographs previously observed in literatures (Sanosh *et al*.2009).

TEM for ground bone powder (Fig. 2) reveals the presence of 2 families of particles, needle-like crystallites of HA (Fig. 2(a)) with needle length lies between 7 and 31nm and a second family of

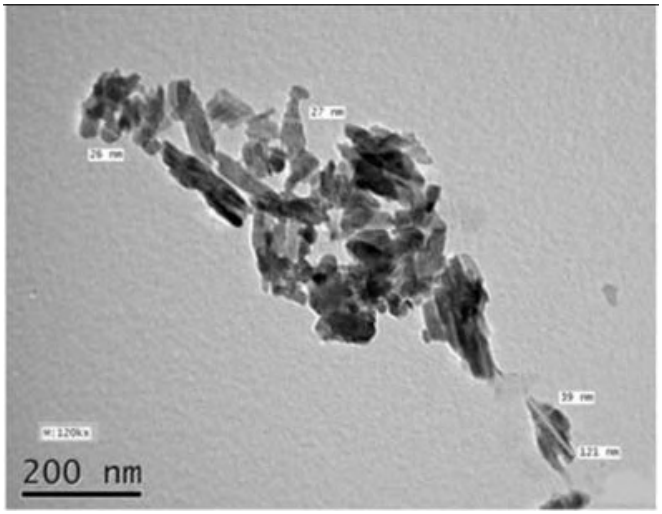

Fig. 1 TEM micrographs of HA

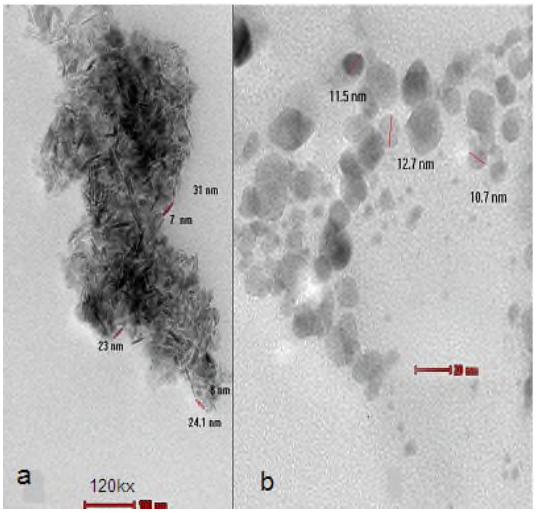

Fig. 2 TEM micrographs of NBP, (a) needle-like crystallites of HA and (b) plate-like crystallites of the NBP

plate-like apatite crystallites (Fig. 2(b)) of about 10-12 nm. TEM studies of animal bones have revealed that regularly arranged hydroxyapatite crystals occur within the collagen matrix in natural bones (Ozawa and Suzuki 2002).

3.2 Transmission electron microscope (TEM)

FTIR spectra of hydroxyapatite (HA) and natural bone powder (NBP) which recorded in the spectral region 4000-400 cm-1 are represented in Fig. 3 and the band assignments are given in Tables 1 and 2.

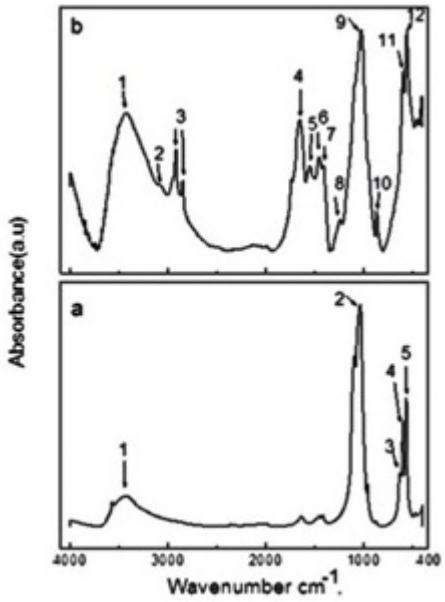

Fig. 3 FTIR of (a) HA and (b) NBP

Table 1 FTIR band assignments for HA

Band No.	Bands (cm^{-1})	Assignments
1	3555	Stretching mode of hydrogen-bonded OH^- ions
2	1031	Stretching mode of PO_4^{-3}.
3	622	Vibrational mode of hydrogen bonded OH^- ions
4	603	Bending mode of PO_4^{-3}.
5	561	Bending mode of $PO_4^{-3.}$

Table 2 FTIR band assignment of NBP

Band No.	Bands (cm^{-1})	Assignments
1	3420	N-H Stretching of amide A
2	3070	Amide B
3	2860-2924	Asymmetric and Symmetric C-H Stretching
4	1654	C=O stretching of amide I
5	1550	N-H bending of amide II
6	1467	Co_3^{-2} vibrations
7	1415	Co_3^{-2} vibrations
8	1240	C-O stretch
9	1032	PO_4^{-3} vibrations
10	870	Co_3^{-2} vibrations
11	603	PO_4^{-3} vibrations
12	566	Bending mode of PO_4^{-2}

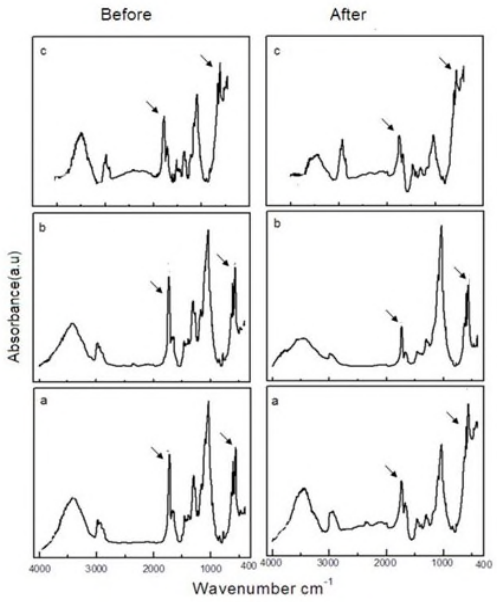

Fig. 4 FTIR spectra of PPF/HA/NBP nanocomposites crosslinked with NVP /MMA and filled with (a) 5 (b) 10 and (c) 15wt% NBP before and after immersion in SBF for 30 days

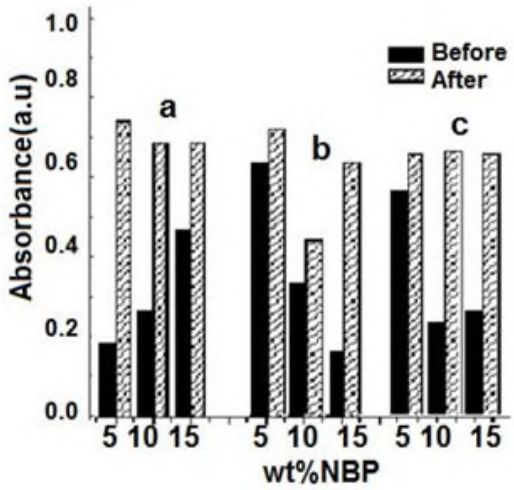

Fig. 5 Intensities of 566cm-1 band for PPF/HA/NBP nanocomposites crosslinked ith (a) MMA, (b) NVP / MMA and (c) NVP and filled with 45wt%HAcontaining (5,10 and15wt%NBP) before and after immersion in SBF for 30 days

PPF/HA/NBP nanocomposites with different crosslinking agents (MMA, NVP/MMA and NVP) and different concentrations of NBP (0, 5, 10 and 15 wt %) were immersed in SBF. The outer layer of the samples was peeled and examined by FTIR spectroscopy before and after immersion for 30 days. The data represented in Fig. 4 for PPF/HA/NBP crosslinked with NVP/MMA as an example.

From the figures it is noticed that, there is a similarity between before and after immersion in SBF and this was expected result when the bioactive layer formed is similar to the filler in the nanocomposites. On the other hand, the change of the intensity of bands and width at half height are connected with the process of hydrolysis of the polymer and the breaking of the bonds in the chain (Chłopek *et al*. 2010). The intensity at 566 cm-1characteristic of the vibration of the phosphate group in the HA was chosen for comparing the intensity before and after immersion in SBF the results are displayed in Fig. 5 for PPF/HA/NBP nanocomposites.

From this figure, it is clear that the intensity of the band at 566 cm-1 was increased. This is a good evidence for the formation of layer of bone apatite layer onto the surface of the investigated samples.

3.3 In-vitro studies during immersion in SBF

3.3.1 Weight loss

Fig. 6 shows the degradation rate of the PPF/HA /NBP crosslinked with MMA, NVP/ MMA and NVP and filled with 10wt%NBP. From this figure it is clear that the degradation rate follow the order MMA>NVP/MMA>NVP.

The effect of increasing the NBP concentration on the degradation rate of PPF/HA/NBP nanocomposites is illustrated in Fig. 7 for nanocomposites crosslinked with NVP as an example. From this figure it is clear that the weight loss decrease by increasing the concentration of the NBP. This decrease in the weight loss may attribute to increasing the content of bone morphogenetic proteins which resulted in high degree of stability in SBF (Haroun and Migonney 2010). It is worth to mention that the rate of degradation of the nanocomposites reinforced with bone powder was significantly slower when compared with those of PPF/HA nanocomposites in our previous study (Kamel *et al*. 2012).

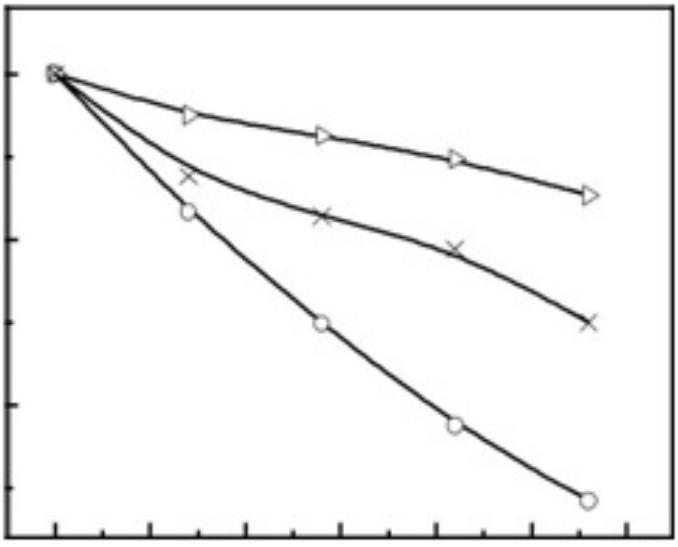

Fig. 6 Degradation rate of PPF/HA/NBP nanocomposites crosslinked with MMA,NVP/MMA and NVP and filled with45wt%HA containing 10 wt% NBP versus time (days)

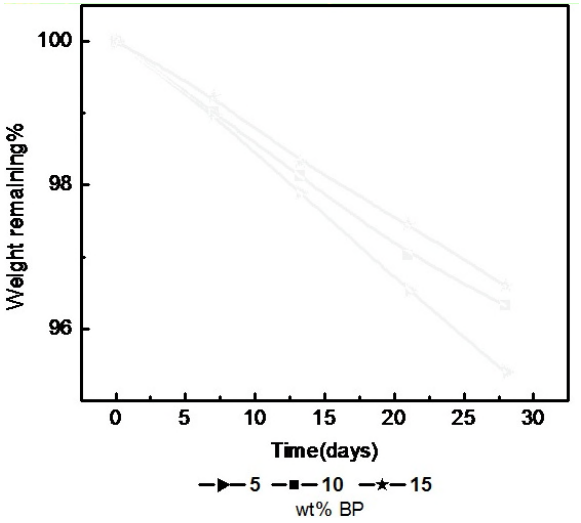

Fig. 7 Degradation rate of PPF/HA/NBP nanocomposites crosslinked with NVP and filled with 45 wt% HA containing 5, 10 and 15wt % NBP versus time (days)

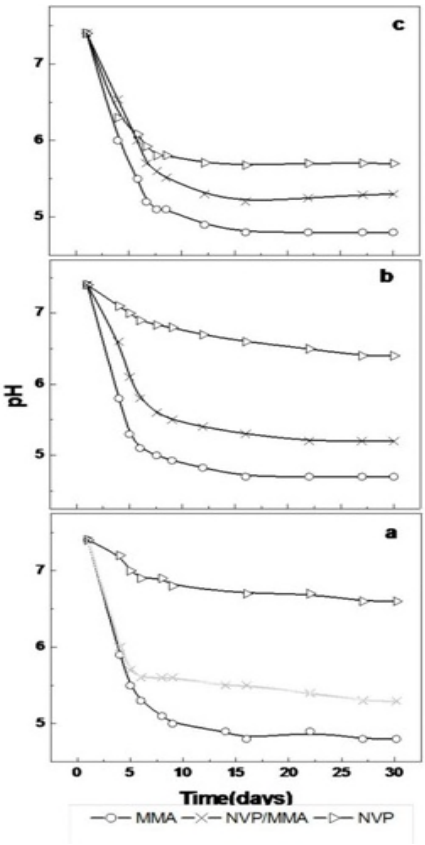

Fig. 8 The changing in the PH values of the SBF during immersion of PPF/HA/NBP nanocomposites crosslinked with MMA, NVP/MMA and NVP and filled with 45wt% HA containing (a) 5, (b) 10and (c) 15wt% NBP

3.3.2 pH measurements

The pH of the SBF solution during immersion of the samples was measured to monitor the changes that could be a combination of acidic degradation byproducts resulting from the polymer and any neutralization effects resulting from the fillers.

The changes of the pH values of the SBF during immersion of PPF/HA/NBP nanocomposites crosslinked with MMA, NVP/MMA and NVP are shown in Fig. 8.

For all samples, the pH of the SBF decreased at the first 3 days of immersion as a result of dissolution of the nanocomposites which suggest high reactivity of these nanocomposites. After that slow decrease in the values noticed till constant values were reached .The lowest values were ranging from 5-6.4. Maruyama and Ito (1996) reported that the exposure of cells to pH 6.0 for 24-48h had no deleterious effects on cell recovery. Therefore, the small pH change produced by PPF/HA/NBP nanocomposites may not have serious effects on cellular functions in addition, the continuous circulation in human body is expected to keep the pH value within an acceptable range.

3.4. Evaluation of the bioactivity of the nanocomposites

3.4.1 Scanning electron microscope (SEM) and energy dispersive X-ray (EDX)

The PPF/HA/NBP nanocomposites crosslinked with MMA, NVP/MMA and NVP, and filled with different concentrations of NBP were immersed in SBF for 30 days. After the period of immersion the nanocomposites filled with 10wt% NBP crosslinked with NVP/MMA are illustrated as an example in Fig. 9. The calcium and phosphorous concentrations before and after immersion are recorded in Table 3.

From the SEM micrograph before immersion in SBF (Fig. 9(a)) there were no cracks which indicate good compatibility between organic and inorganic phases.

During immersion in SBF roughness in surface of all the samples can be observed. The

Table 3 Calcium and phosphorous concentrations for the PPF/HA/NBP nanocomposites crosslinked with MMA, NVP and NVP/MMA and filled with 45wt%HA containing 10 wt% NBP before and after immersion in SBF for 30 days.

Element	Concentrations of elements (at. %)	
	Before immersion	After immersion
PPF/HA/NBP crosslinked with MMA		
Phosphorus	6.31	7.61
Calcium	9.66	11.98
Molar Ca/p ratio	1.53	1.57
PPF/HA/NBP crosslinked with NVP/MMA		
Phosphorus	5.51	18.40
Calcium	9.72	31.53
Molar Ca/p ratio	1.76	1.71
PPF/HA/NBP crosslinked with NVP		
Phosphorus	3.81	5.94
Calcium	6.06	10.74
Molar Ca/p ratio	1.59	1.8

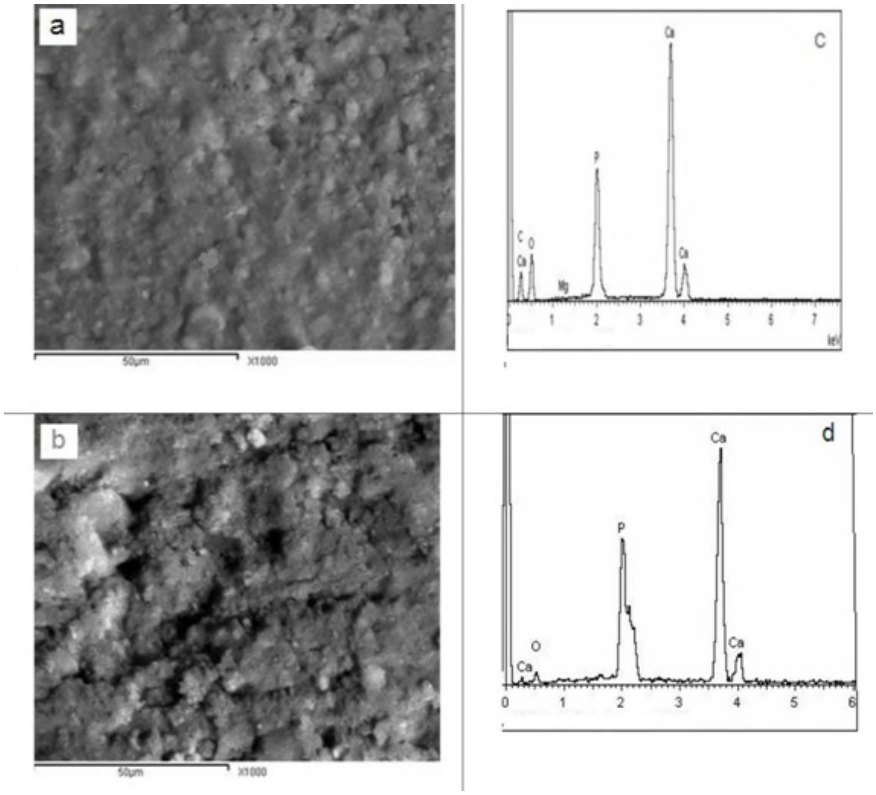

Fig. 9 SEM micrograph and EDX spectrum of PPF/HA/NBP samples crosslinked with NVP/MMA and filled with 45wt% HA containing 10 wt% NBP (a and c) before, (b and d) after immersion in SBF for 30 day

roughness increases with increasing the immersion time and the surface began to exhibit surface pores due to the degradation of the polymer. The degradation of the polymer results in more exposure of the bioactive HA and NBP fillers to the SBF leading to nucleation of the bioactive calcium phosphate layer by consuming the calcium and phosphorous ions from the solution.

After 30 days of immersion the surfaces was analyzed by scanning electron microscope (Fig. 9(b)) .The bioactivity of the nanocomposites was confirmed by the presence of small and large spherical particles with bright color denoting deposition of calcium phosphate particles which coated all the surfaces. The EDX spectra before immersion (Fig. 9(c)) revealed the presence of carbon (C) and oxygen (O2) of the polymer, calcium (Ca), phosphorous (P), sodium (Na) and magnesium (Mg) as a result of incorporation of the bone powder (Miculescu *et al*. 2011) After immersion for 30 days in SBF (Fig. 9(d)) the EDX analysis revealed the presence of the same elements with increases in both calcium and phosphorous signals. The phosphocalcic ratio was 1.57, 1.71 and 1.8 for PPF/HA/NBP crosslinked with MMA, NVP/MMA and NVP respectively which is comparable with the stoichiometries apatite

3.5 Dielectric measurements

The frequency dependence of the permittivity ε′ and dielectric loss ε" over the frequency range from 100 Hz-100 kHz and at 30°C for poly(propylene fumarate) (PPF) crosslinked with different

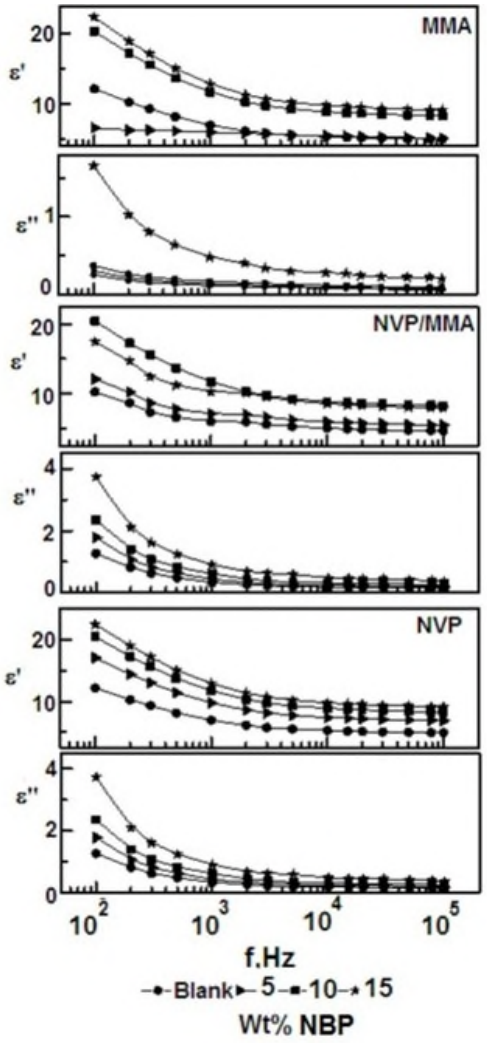

Fig. 10 The permittivity ε' and dielectric loss ε'' versus frequency f of PPF/HA/NBP nanocomposites crosslinked with MMA, NVP/ MMA and NVP and filled with 45wt% HA containing 5, 10 and 15wt% NBP

crosslinking agents NVP, MMA and NVP/MMA and their nanocomposites with a fixed amount of HA 45% containing different concentrations of NBP (5, 10 and 15wt %). The obtained data are illustrated graphically in Fig. 10.

From this figure, it is seen that ε′ for all investigated samples decreases with increasing the frequency, which shows anomalous dispersion. The rotational motion of the polar molecules of dielectric is not sufficiently rapid for attain equilibrium with the field (Pathania and Singh 2009). This behavior is expected in most polymers dielectrics and is due to the dielectric relaxation phenomena of the polymer materials. Within the measured frequency range, the dielectric relaxation involves the dipolar (rotational) polarization, which depends on the molecular structure of the material. At higher frequencies, the rotational motion of the molecules lags behind the electric field, leading to reduced permittivity with increasing frequency (Zhan *et al*. 2011). Such

high values of ε′ may be due to the interface effects within the bulk of the sample and the electrode effects and or Maxwell Wagner polarization (Ramesh *et al.* 2002, Sengwa and Sankhla 2007). The values of both ε′and ε" are found to be comparable with those found before in literature (Kamel *et al*. 2010).

It is also clear that the values of ε′ and ε" increase in the order MMA < NVP/MMA < NVP. This is may be due to the higher polarity of NVP, (4D) (Hu *et al*. 2000) compared with that of MMA, (1.79 D) (Abd-El-Messieh 2002).

On the other hand, the absorption curves of ε" versus the frequency f shown in Fig. 10 are broad indicating that, in addition to the electrical conductivity, more than one relaxation mechanism is present (Amor *et al*. 2009). After subtracting the conductivity term, the analysis of the absorption curves was done in terms of superposition of Fröhlich function distribution parameter p=3 and a Havriliak-Negami function with distribution parameter α=0.5 and β=0.5 according to the equations given elsewhere (Abd-El-Messieh and Abd-El-Nour 2003). The obtained data are given in Table 4.

The first relaxation process, which was ascribed to the Maxwell-Wagner effect, was found to be on the order of 300 Hz and was unaffected by either filler loading or particle size. Its ε" maximum frequency values were found to increase with increasing filler loading, as shown in Table 4.

The second absorption region in the higher frequency range could be associated with some local molecular motions rather than the main chain motion as it is expected to be frozen because the measurements were carried out at 30^{o}C i.e., lower than the glass transition Tg of the crosslinked polyester (Mc Morrow *et al*. 2003). This relaxation corresponds to the terminal polar groups, carboxyl and hydroxyl functions, and to ester functions in the polymer chain (Havriliak and Havriliak 1997).

Table 4 Relaxation parameters for PPF/HA/NBP nanocomposites crosslinked with MMA, NVP/MMA and NVP filled with 45wt%HA containing 5, 10 and 15wt%NBP

NBP content wt%	□□□□□□□□□x10^{-5}(s)	S2	□□x10^{-11}(S/m)
	PPF/HA/NBP crosslinked with MMA		
0	3.79	0.409	1.1
5	4.48	0.522	1.3
10	5.31	0.640	1.5
15	5.71	0.795	1.8
	PPF/HA/NBP crosslinked with NVP/MMA		
0	2.1	0.722	3.9
5	3.5	0.84	4.64
10	3.9	1.05	6.3
15	4.4	1.42	7.66
	PPF/HA/NBP crosslinked with NVP		
0	1.80	0.986	7.4
5	3.10	1.33	8.7
10	5.01	1.83	11.4
15	5.30	2.85	18.2

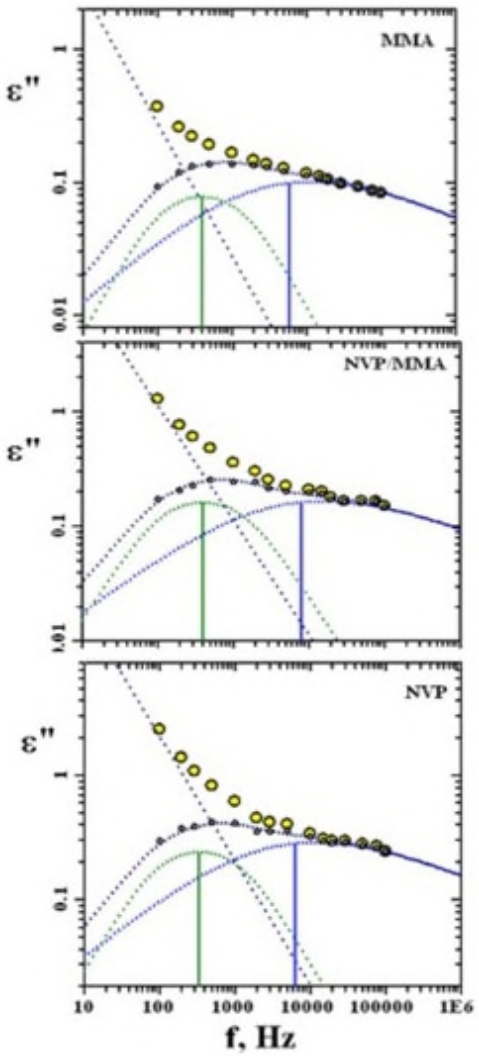

Fig. 11 Example of the analysis for PPF/HA/NBP nanocomposites crosslinked wit NVP/MMA and NVP and filled with 45wt% HA containing10 wt% NBP .The data are fitted by Fröhlich and Havrilliak Negami Functions in addition to the conductivity term respectively

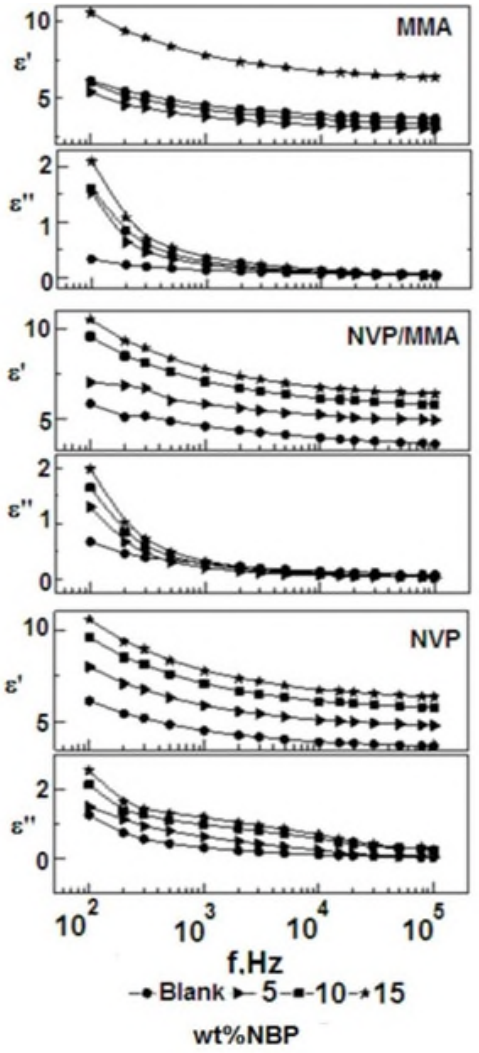

Fig. 12 The permittivity ε′ and dielectric loss ε" versus frequency f of PPF/HA/NBP nanocomposite crosslinked with MMA, NVP/ MMA and NVP and filled with 45wt%HA containing (5, 10 and 15wt% NBP) after immersion in SBF for 30 days

The relaxation time associated with this region is found to be highly affected by the type of crosslinking agent and follows the order MMA > NVP/MMA >NVP i.e. depending on the molar volume of the rotating unites and consequently the on relaxation time (Kamel *et al*. 2010). Example of the analyses for all nanocomposites filled with 45 wt% HA and 10wt%NBP is given in Fig. 11.

After immersing the crosslinked samples in SBF solution for 30 days, the permittivity ε′ and dielectric loss ε" were re-measured and given in Fig. 12. Comparing the data obtained before and after immersing in SBF (Figs. 10 and 12) it is seen that both ε′ and ε" decrease by immersing in the

SBF solution.

This decrease could be due to the formation of apatite structure that takes some ions to crystal formation where they are no longer mobile and no longer contributing to the dielectric spectrum (Mohamed *et al*. 1998). The curves relating ε"and the applied frequency were analyzed into one process by using Havriliak Negami function in addition to the conductivity term. This is because the fact that value of τ_2 becomes large and consequently that the electrical conductivity becomes predominant rather than Maxwell Wagner effect. The obtained relaxation data are listed in Table 4. Example of the analyses is given in Fig. 11 for NVP filled with 45wt% HA containing 10wt% bone before and after immersing in SBF solution.

Comparing Tables 4 and 5 it is interesting to find that both conductivity and S2 decrease while a pronouncing increase in 2 is noticed. The increase in 2 reflects an increase in the molar volume of the rotating unites due to the formation of apatite structure that takes some ions to crystal formation to become no longer mobile and thus no longer contributing to dielectric spectrum. In order to find an expression to distinguish between the amounts of apatite structure which is assumed to be formed by immersing the investigated samples in SBF, the relation (aft.- bef.)/ bef was calculated and listed in Table 5. From this table it is interesting to notice that the values of (aft.- bef..)/ bef increase by the addition bone up tell 10 wt% after which a slight increase was noticed at concentration 15wt% this increase was found to follow the order NVP>NVP/MMA >MMA. This finding is found to be comparable with that found before in case of PPF/gypsum nanocomposites (Kamel *et al*. 2010).

3.6 Mechanical analysis

The mechanical behavior under compressive forces was studied through the compressive

Table 5 Relaxation parameters for PPF/HA/NBP nanocomposites crosslinked with MMA, NVP/MMA and NVP and filled with 45wt%HA containing 5, 10 and15 wt% NBP after immersion in SBF for 30 days

NBP content wt%	τ2x10-5(s)	S2	σ x 10-11(S/m)	(τaft - τ bef) / τbef
PPF/HA/NBP crosslinked with MMA				
0	11.00	0.198	1.35	1.9
5	14	0.297	6.27	2.13
10	19	0.432	8.75	2.58
15	21	0.561	14.00	2.68
PPF/HA/NBP crosslinked with NVP/MMA				
0	8.8	0.637	3.00	3.19
5	16.01	0.287	7.16	3.57
10	20.12	0.375	9.05	4.13
15	23.02	0.469	10.70	4.05
PPF/HA/NBP crosslinked with NVP				
0	8.73	0.394	6.48	3.85
5	15.50	0.709	8.52	4.17
10	26.25	2.83	13.5	4.25
15	28.00	3.62	11.8	4.28

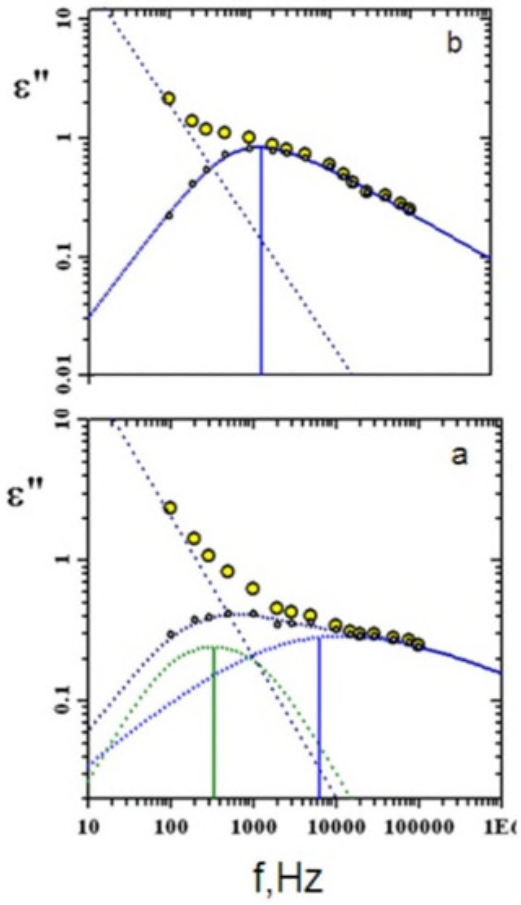

Fig. 13 Example of the analysis for PPF/HA/NBP nanocomposites crosslinked with NVP and filled with 45wt%HA containing 10wt%NBP(a) before and (b) after immersion in SBF for 30 days .The data are fitted by using Fröhlich and HavriliakNegami Functions respectively

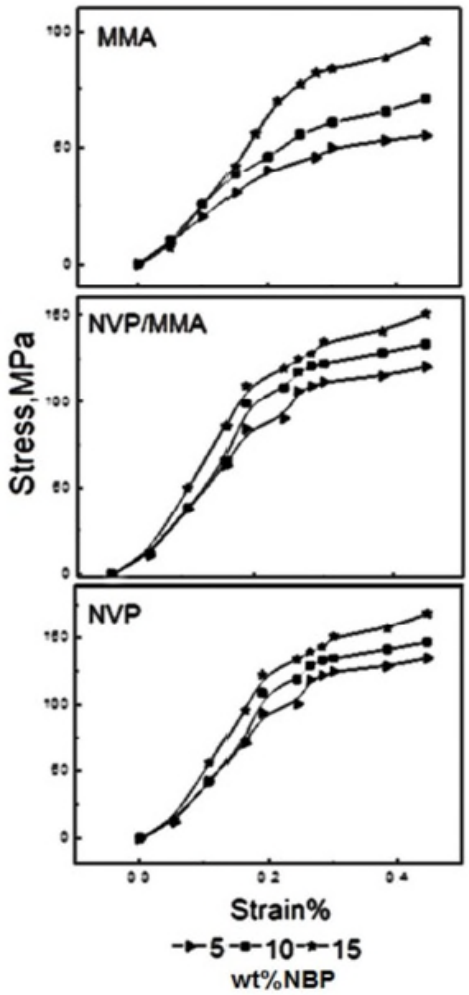

Fig. 14 Compressive stress–strain diagram of PPF/HA/NBP nanocomposites crosslinked with MMA, NVP/MMA and NVP and filled with 45wt%HA containing 5, 10 and 15 wt % NBP before immersion in SBF for 30 days

strength at fracture. It is defined as the maximum stress carried by the specimen during the test "the peak of the stress-strain curve" (He *et al*. 2001).

The compressive stress-strain diagrams for the fumarate resin crosslinked with MMA, NVP/MMA and NVP and filled with 45wt% HA containing different concentrations of NBP (5, 10 and 15wt %) are given in Fig. 14. From the figure it is clear that the incorporation of bone powder to the PPF /HA nanocomposites resulted in significant increase in the values of compressive strength .The compressive stress was 139.89, 127.66 and 65.82 Mpa at strain 0.36% for composite filled with 45wt%HA containing 10wt% NBP and crosslinked with NVP, NVP/MMA and MMA respectively.

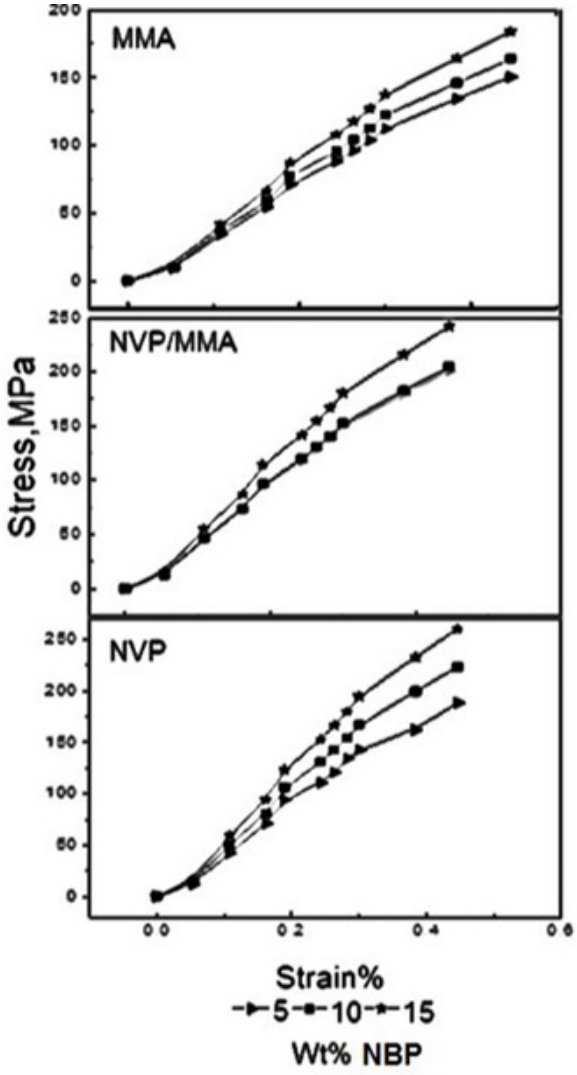

Fig. 15 Compressive stress–strain diagram of PPF/HA/NBP nanocomposites crosslinked with MMA, NVP/MMA and NVP and filled with 45wt%HA containing5, 10 and 15 wt % NBP after immersion in SBF for 30 days

After immersion the nanocomposites in SBF for 30 days (Fig. 15) the values of the compressive strength increase to reach 190.37, 175.70 and 140.81 MPa at strain 0.36% for nanocomposites filled with 10wt% NBP and crosslinked with NVP, NVP/MMA and MMA respectively. The mechanical properties of poly (propylene fumarate) (PPF)-based composite material increased with degradation time, which was explained by a crosslinking effect promoted by complexation between carboxylic groups, formed from PPF degradation and accumulated in the incubation solution, with divalent calcium ions released from hydroxyapatite (Yaszemski *et al.* 1996).The results suggest that PPF/HA/NBP nanocomposites with a wide range of mechanical properties could be applied for different clinical uses.

4. Conclusions

• Trying to enhance the biological and mechanical properties of the PPF/HA nanocomposites, different concentrations of chemically treated bone powder (NBP) (5,10 and15wt%) was incorporated into the PPF/HA 45wt% composite. The FTIR spectra of the NBP samples revealed the characteristic peaks of a residual organic matrix in addition to the characteristic peaks of the bone apatite phase (CO3-2 and PO4-3). After immersion in the SBF, the increase in the intensities of the bands at wave numbers 1030, 566cm-1for phosphate group were more pronounced and confirmed the bioactivity of such nanocomposites.

• The SEM images and phosphocalcic ratio confirmed that the layer formed on the surface of the nanocomposites is hydroxyapatite. From the dielectric spectra, after immersion in SBF both conductivity and S2 decrease while a pronouncing increase in $\tau 2$ is noticed. The increase in $\tau 2$ reflects an increase in the molar volume of the rotating unites due to the formation of apatite structure.

• From the mechanical analysis it is found that the incorporation of bone powder to the PPF /HA nanocomposites resulted in significant increase in the compressive strength .The compressive strength was 139.89, 127.66 and 65.82 Mpa at strain 0.36% for composite filled with 10wt% NBP and crosslinked with NVP, NVP/MMA and MMA respectively.

• The degradation rate of these nanocomposites decrease by increasing the bone powder content. The PH of the SBF solution during immersion the nanocomposites was monitored and found to be ranging from 5- 6.4.

From the previous results it is concluded that, addition of different concentrations of natural bone powder to PPF/HA 45wt% nanocomposites leads to: enhancement bioactivity and the mechanical properties ,decreasing the degradation rate which lead to stability of these nanocomposites, produce less change in the pH of the SBF solution during the immersion of the nanocomposites. The results could recommend the NVP/MMA to be used in crosslinking polypropylene fumarate rather than the expensive monomer NVP and the unrecompensed one MMA. The PPF/HA/NBP nanocomposites are ideal for bone tissue regeneration. The effectiveness of the dielectric tool for such studies.

References

Abd-El-Messieh, S.L. (2002), "Dielectric relaxation of binary systems of some disubstituted fumarates with acrylonitrile and vinylacetate in CCl 4 solutions", *J. Mol. Liq.*, **95**(2), 167-182.

Abd-El-Messieh, S.L. and Abd-El-Nour, K.N. (2003), "Effect of curing time and sulfur content on the dielectric relaxation of styrene butadiene rubber", *J. Appl. Polym. Sci.*, **88**(7), 1613-1621.

Amor, I.B., Rekik, H., Kaddami, H., Raihane, M., Arous, M and Kallel, A. (2009), "Studies of dielectric relaxation in natural fiber–polymer composites", *J. Electrostat*, **67**(5), 717-722.

Chłopek, J., Morawska-Chochół, A. and Szaraniec, B. (2010), "The influence of the environment on the degradation of polylactides and their composites", *J. Achv. Mater. Manuf. Eng.*, **43**(1), 72-79.

Fantner ,G.E. *et al*. (2004), "Influence of the degradation of the organic matrix on the microscopic fracture behavior of trabecular bone", *Bone*, **35**, 1013-1022.

Gaharwar, A.K., Schexnailder, P.J. and Schmidt, G. (2011), "Nanocomposite polymer biomaterials for tissue repair of bone and cartilage", *A Material Science Perspective Nanomaterial, Nanobiomaterials Handbook*, Ed. B. Sitharaman, CRC Press, Chapter 24.

Haroun, A.A. and Migonney, V. (2010), "Synthesis and in vitro evaluation of gelatin/hydroxyapatite

graftcopolymers to form bionanocomposites", *J. Biol.Macromol.*, **46**(3), 310-316.
Havriliak, S. and Havriliak, S.J. (1997), *Dielectric and mechanical relaxation in materials: analysis, interpretation and application to polymers*, Hanser, New York.
He, S., Timmer, M.D., Yaszemski, M.J., Yasko, A.W., Engel, P.S. and Mikos, A.G. (2001), "Synthesis of biodegradable poly (propylene fumarate) networks with poly (propylene fumarate)-diacrylate macromers as crosslinking agents and characterization of their degradation products", *Polymer*, **42**(3), 1251-1260.
Horch, R.A., Shahid, N., Mistry, A.S., Timmer, M.D., Mikos, A.G. and Barron, A.R. (2004), "Nanoreinforcement of poly (propylene fumarate)-based networks with surface modified alumoxane nanoparticles for bone tissue engineering", *Biomacromol.*, **5**(5), 1990-1998.
Hu, Y., Motzer, H.R., Etxeberria, A.M., Fernandez-Berridi, M.J., Iruin, J.J., Painter, P.C and Coleman, M. M. (2000), "Concerning the self-association of N-vinyl pyrrolidone and its effect on the determination of equilibrium constants and the thermodynamics of mixing", *Macromol. Chem. Phys.*, **201**(6), 705-714.
Jayabalan, M., Shalumon, K.T., Mitha, M.K., Ganesan, K. and Epple, M. (2010), "Effect of hydroxyapatite on the biodegradation and biomechanical stability of polyester nanocomposites for orthopaedic applications", *Acta Biomater.*, **6**(3), 763-775.
Johnson, G.S., Mucalo, M.R., Lorier, M.A., Gieland, U. and Mucha, H. (2000), "The processing and characterization of animal-derived bone to yield materials with biomedical applications. Part II: milled bone powders, reprecipitated hydroxyapatite and the potential uses of these materials", *J. Mat. Sci.: Mat. Med.*, **11**(7), 727-741.
Kamel, N.A., Abou Aiaad, T.H., Iskander, B.A., Khalil, S.K.H., Mansour, S.H., Abd El-Messieh, S.L. and Abd El-Nour, K.N. (2010), "Biophysical studies on bone cement composites based on polyester fumarate", *J. Appl. Polym. Sci.*, **116**(2), 876-885.
Kamel, N.A., Abd-El-Messieh, S.L., Mansour, S.H., Iskander, B.A., Khalil, W.A. and Abd-El-Nour, K.N. (2012), "Biophysical properties of crosslinked poly (propylene fumarate)/hydroxyapatite nanocomposites", *Rom. J. Biopys*, **22**(3-4), 189-214.
Langer, R. and Vacanti, J.P. (1993), "Tissue engineering", *Science*, **260**, 920-926.
Lee, J.W., Lan, P.X., Kim, B., Lim, G. and Cho, D.W. (2008a), "Fabrication and characteristic analysis of a poly (propylene fumarate) scaffold using micro stereolithography technology", *J. Biomed. Mater. Res. B*: *Appl. Biomater.*, **87**(1), 1-9.
Lee, K.W., Wang, S., Yaszemski, M.J. and Lu, L. (2008b), "Physical properties and cellular responses to crosslinkable poly (propylene fumarate)/hydroxyapatite nanocomposites", *Biomaterials*, **29**(19), 2839-2848.
Maruyama, M. and Ito, M. (1996), "In vitro properties of a chitosan bonded self hardening paste with hydroxyapatite granules", *J. Biomed. Mater. Res.*, **32**(4), 527-532.
Ma, P.X. (2004), "Scaffolds for tissue fabrication", *Mater. Today*, **7**, 30-40.
Ma, P.X. (2005), "Tissue engineering", *Encyclopedia of Polymer Science and Technology*, Eds. Kroschwitz JI, John Wiley & Sons, Inc., Hoboken, NJ.
Ma, P.X. (2008), "Biomimetic materials for tissue engineering", *Adv. Drug Deliv. Rev.*, **60**(2), 184-198.
McMorrow, R.C. and Klosterman, D. (2003), "Advancing materials in the global economy-applications", *Emerging Markets and Evolving Technologies International Symposium and Exhibition*, Long Beach, CA, May.
Mohamed, M.G., Abd-El-Messieh, S.L., El-Sabbagh, S. and Younan, A.F. (1998), "Electrical and mechanical properties of polyethylene-rubber blends", *J. Appl. Polym. Sci.*, **69**(4), 775-783.
Ozawa, M. and Suzuki, S. (2002), "Microstructural development of natural hydroxyapatite originated from fish bone waste through heat treatment", *J. Am. Ceram. Soc.*, **85**(5), 1315-1317.
Pathania, D. and Singh, D. (2009), "A review on electrical properties of fibre reinforced polymer composites", *Int. J. Theor. Appl. Sci.*, **1**(2), 34-37.
Ramesh, S., Yahaya, A.H. and Arof, A.K. (2002), "Dielectric behaviour of PVC-based polymer electrolytes", *Solid. State. Ionics.*, **152**, 291-294.
Sengwa, R.J. and Sankhla, S. (2007), "Dielectric dispersion study of coexisting phases of aqueous polymeric solution: Poly (vinyl alcohol)+poly (vinyl pyrrolidone) two-phase systems", *Polymer*, **48**(9), 2737-2744.

Shi, X., Hudson, J.L., Spicer, P.P., Tour, J.M., Krishnamoorti, R. and Mikos, A.G. (2006), "Injectable nanocomposites of single-walled carbon nanotubes and biodegradable polymers for bone tissue engineering", *Biomacromol.*, **7**(7), 2237-2242.

Temenoff, J.S., Kasper, F.K. and Mikos, A.G. (2007), "Fumarate-based macromers as scaffolds for tissue engineering applications", *Topics in Tissue Engineering*, Eds. R. Reis, E. Chiellini, **3**, 1-16.

Timmer, M.D., Ambrose, C.G. and Mikos, A.G. (2003), "In vitro degradation of polymeric networks of poly (propylene fumarate) and the crosslinking macromer poly (propylene fumarate)-diacrylate", *Biomater.*, **24**(4), 571-577.

Yaszemski, M.J., Payne, R.G., Hayes, W.C., Langer, R. and Mikos, A.G. (1996), "In vitro degradation of a poly (propylene fumarate)-based composite material", *Biomater.*, **17**(22), 2127-2130.

Zhan, M., Wool, R.P. and Xiao, J.Q. (2011), "Electrical properties of chicken feather fiber reinforced epoxy composites", *Compos. Part A: Appl. Sci. Manuf.*, **42**(3), 229-233.

CC